

# Millimeter-Wave Electromagnetic Field Measurement Based on LiNbO<sub>3</sub> Optical Modulator Using Patch Antennas Embedded with Gaps

Yusuf Nur WIJAYANTO<sup>1</sup>, Hiroshi MURATA<sup>2</sup>, Atsushi KANNO<sup>1</sup>,  
Tetsuya KAWANISHI<sup>1</sup>, and Yasuyuki OKAMURA<sup>2</sup>

<sup>1</sup> Lightwave Device Laboratory, Photonic Networks Research Institute,  
National Institute of Information and Communications Technology

4-2-1 Nukui-Kitamachi, Koganei, Tokyo 184-8795 Japan

<sup>2</sup> Graduate School of Engineering Science, Osaka University

1-3 Machikaneyama, Toyonaka, Osaka, 560-8531 Japan

E-mail: ynwijayanto@nict.go.jp

**Abstract:** Millimeter-wave electromagnetic field (EMF) measurement based on a LiNbO<sub>3</sub> optical modulator using patch antennas embedded with gaps is proposed. In this method, millimeter-wave characteristics of a device under test (DUT) can be detecting using the proposed EMC sensor and measured by adopting radio-over-fiber (ROF) technology. As basic operation, wireless millimeter-wave EMF irradiation from a DUT can be identified by use of the patch antennas and converted to lightwave directly by use of the LiNbO<sub>3</sub> optical modulator through electro-optic (EO) modulation. The converted lightwave can be propagated to optical fibers with low propagation loss. The induced millimeter-wave induction and losses can be minimized since no other metal planar structures on the EMF sensor except the patch antennas. Therefore, precise measurement of the millimeter-wave electric fields can be obtained. In this report, structure and analysis of the EMF sensor based on a LiNbO<sub>3</sub> optical modulator using patch antennas embedded with gaps are discussed in detail for 40GHz millimeter-wave bands. Furthermore, experimental methods and results for millimeter-wave EMF measurement are also reported.

**Keywords:** Electromagnetic field measurement, millimeter-wave bands, LiNbO<sub>3</sub> optical modulator, patch antenna, radio-over-fiber.

## 1. Introduction

EMC is abbreviation of Electro-Magnetic Compatibility, which is the ability of an electronic device or system to function properly without generating pollution to the electromagnetic environment [1]. Any electronic equipment must be measured their electromagnetic field (EMF) radiation and susceptibility. Therefore, they can work properly without any interference each other.

Recently, mobile devices are widely used with wireless technology [2]. EMF in operational frequencies of mobile devices are available in the air/ space. In this time, microwave band is widely used. In order to follow EMC standard regulation of each country, the mobile devices should be checked and measured their characteristics to avoid the interference.

EMF measurement is done usually in an EMC chamber [3,4]. It can be composed of an antenna, cable, and measurement tools such as a signal generator, amplifier,

power meter, spectrum analyzer, oscilloscope, and so on. The device characteristics of EMF such as magnitude, phase, and polarization are observed. A device under test (DUT) and observation rooms are separated with a distance. The antenna and measurement tools are connected using a coaxial cable. Since microwave bands are operated for the system, microwave losses and distortion might be no big issues. Additionally, unwanted environmental noises and interferences might be induced to the system [5].

In order to anticipate future mobile technology in millimeter-wave bands (30–300GHz) with wide broadband wireless access, a system for EMF measurement should be prepared also. In millimeter-wave bands, large propagation losses and precise tuning are big problem to solve [6]. They can be solved by adopting radio-over-fiber (ROF) technology. By using the ROF technology, a millimeter-wave EMF can be converted to lightwave. Then, the lightwave is propagated through an optical fiber. Finally,

the lightwave is reconverted to millimeter-wave for measuring its characteristics. The optical fiber has very low propagation losses and immune to environmental EMF noises [7]. Therefore, precise EMF measurement in millimeter-wave bands can be obtained using the ROF technology.

In the millimeter-wave ROF technology, converters between millimeter-wave and lightwave signals are required. For millimeter-wave EMF transmitter, a high-speed photo-detector is used for converting a lightwave to millimeter-wave EMF [8]. On the other side for millimeter-wave EMF receiver/ sensor, a high-speed optical modulator is used for converting a millimeter-wave to lightwave [9].

The high-speed optical modulator for millimeter-wave bands can be composed of millimeter-wave antennas and optical modulation electrodes with connection lines. They can be arranged discretely [10]. However, millimeter-wave distortion might occur and mismatching condition due to. It can be reduced using an optical modulator with antennas integrated with resonant electrodes in a compact device structure [11]. In the integrated structures, precise tuning is rather difficult to obtain due to small operational wavelength, as a result the millimeter-wave distortion might be still induced in small value.

In this report, a LiNbO<sub>3</sub> optical modulator using patch antennas embedded with gaps is proposed for millimeter-wave EMF measurement. The patch antennas are fabricated on a LiNbO<sub>3</sub> modulator for identifying millimeter-wave EMF and converting the received millimeter-wave to lightwave through the electro-optic (EO) effects of the LiNbO<sub>3</sub> crystal. Magnitude, polarization, and phase of the millimeter-wave EMF can be observed using the proposed EMF sensor with ROF technology.

In the following sections, structure and analysis of the proposed EMF sensor are discussed for 40GHz millimeter-wave bands. The experiment methods and its results for millimeter-wave EMF measurement are also reported.

## 2. Structure of EMF Sensor

Figure 1 shows the structure of the proposed millimeter-wave EMF sensor. It is composed by patch antennas embedded with gaps fabricated on a low- $k$  dielectric substrate and optical waveguides fabricated on a LiNbO<sub>3</sub> optical crystal. They are bonded each other. The patch antennas embedded with very narrow gaps are fabricated by gold metal, where the patch length ( $L$ ) is set to half wavelength of the designed millimeter-wave. The optical waveguides are located on a one side of the gap

edge as shown in Fig. 1(b). A SiO<sub>2</sub> buffer layer is inserted between the LiNbO<sub>3</sub> optical crystal and patch antennas.

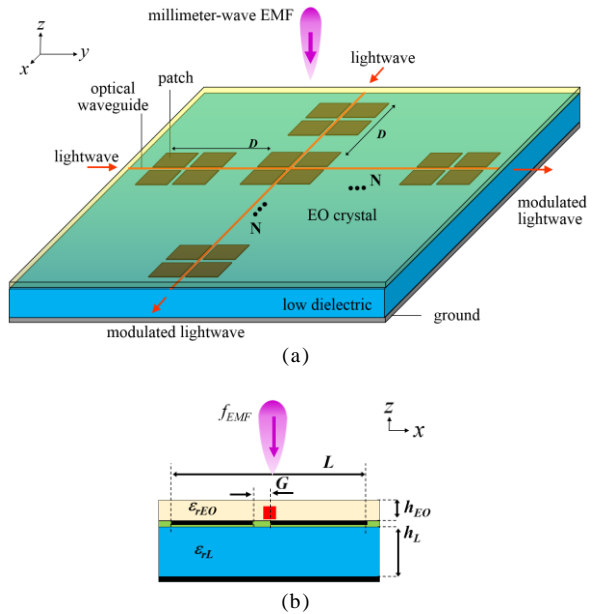


Fig. 1 Structure of the proposed millimeter-wave EMF sensor (a) whole, and (b) cross-sectional views.

When millimeter-wave EMF is radiated by a DUT and then received by the proposed sensor, standing-wave current of millimeter-wave electric field is induced on the patches. By introducing gaps on the patches, displacement current is induced across the gaps for current flow continuity [12]. Simultaneously, the strong millimeter-wave electric field is also induced across the gaps. The strong millimeter-wave electric field across the gaps can be used for EO modulation through the Pockels effects [13]. When lightwave propagates to the optical waveguides, optical modulation is obtained from the lightwave outputs. Therefore, the millimeter-wave EMF can be identified, received, and converted to lightwave directly using the proposed EMF sensor. Based on this, the magnitude and phase of the millimeter-wave EMF can be measured. Additionally, since the proposed EMS sensor is composed of orthogonal optical waveguides and patch antenna embedded with orthogonal gaps, the polarization of the EMF can be also observed by comparing between the modulated lightwave from the orthogonal waveguides.

## 3. Analysis of EMF Sensor

Basically, the proposed EMF sensor is patch antennas with narrow gaps. Design rule for standard patch antennas was reported in many books and papers [14, 15]. The patch antennas can be designed by setting its length and

considering its effective dielectric constant. Additionally, the displacement current and strong electric field across the narrow gaps were also discussed.

The proposed EMF sensor was designed and analysis by use of electromagnetic analysis software (HFSS). The parameters of the proposed EMF sensor for 40GHz millimeter-wave bands are shown in Table 1.

Table 1 Parameters of the proposed EMF sensor.

| Parameter  | Value       |
|--|-------------|
| EMF operational frequency                                      | ~40GHz      |
| EO crystal   |             |
| • z-cut LiNbO <sub>3</sub>                                     |             |
| • Dielectric constant ( $\epsilon_x, \epsilon_y, \epsilon_z$ ) | (41,41,28)  |
| • Thickness ( $h_{EO}$ )                                       | ~70 $\mu$ m |
| Low- $k$ dielectric contant                                    |             |
| • MCL-FX2  |             |
| • Dielectric constant ( $\epsilon_{rL}$ )                      | 3.5         |
| • Thickness ( $h_L$ )  | 130 $\mu$ m |
| Patch antenna with gaps  |             |
| • Gold material  |             |
| • Patch size ( $L \times L$ )                                  | 1.6x1.6mm   |
| • Gap width ( $G$ )  | 10 $\mu$ m  |
| • Thickness  | 2 $\mu$ m   |
| • Distance in array ( $D$ )                                    | 2.3mm       |
| Buffer layer   |             |
| • Thickness  | 0.2 $\mu$ m |

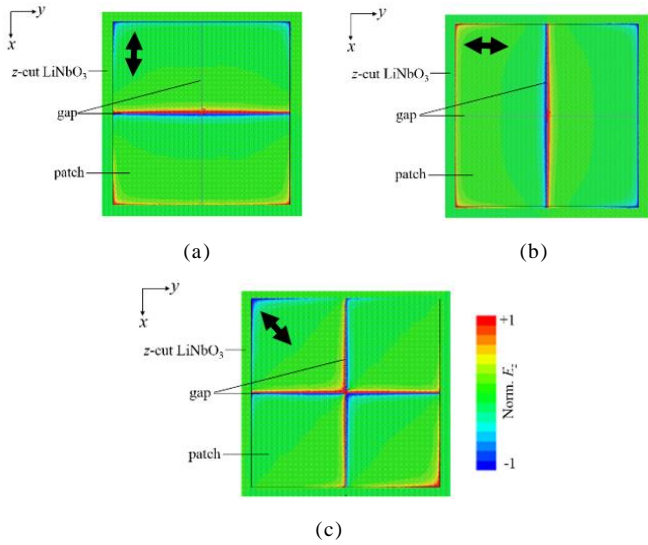


Fig. 2 Electric field distribution on the substrate surface with polarization variations: (a) along x-axis, (b) along y-axis, and (c) 45 degrees between x- and y-axes.

Figure 2 shows the calculated millimeter-wave electric field distributions on the substrate surface when millimeter-wave EMF for variations of millimeter-wave polarizations is irradiated to the proposed EMF sensor. We can see that the strongest electric field is induced across a gap when the irradiated millimeter-wave polarization is perpendicular to the gap. In contrary, when the irradiated millimeter-wave polarization is parallel to a gap, there is

no electric field across the gap. Additionally, when millimeter-wave polarization is not completely perpendicular or parallel to the gaps as shown in Fig. 2(c), strong electric fields are induced across the orthogonal gaps.

Based on the characteristics, the millimeter-wave EMF from a DUT can be identified using patch antennas with orthogonal gaps. The magnitude and polarization of the millimeter-wave EMF can be observed clearly by comparing the induced electric field across the gaps. Furthermore, the induced millimeter-wave electric field can be used for optical modulation through Pockels effect.

In order to analyze modulation efficiency through EO modulation from orthogonal optical waveguides, the transit-time effect must be considered [16]. The transit-time effects along x- and y-axes are expressed as following equations,

$$\text{along } x\text{-axis: } x' = x - v_g t \quad (1)$$

$$\text{along } y\text{-axis: } y' = y - v_g t \quad (2)$$

where  $x'$  and  $y'$  denote the point of the lightwave in the coordinate system moving with the lightwave, and  $v_g$  is the group velocity of the lightwave.

In an array structure, the millimeter-wave electric fields observed by lightwave at the  $h$ -th patch can be expressed as following equations,

from waveguide along x-axis:

$$E_{light}^h(x) = E_0 \cos(k_m n_g x) + hD(k_m n_0 \sin \theta_x + \varphi) \quad (3)$$

from waveguide along y-axis:

$$E_{light}^h(y) = E_0 \cos(k_m n_g y) + hD(k_m n_0 \sin \theta_y + \varphi) \quad (4)$$

where  $n_g$  is the group index of the lightwave propagating in optical waveguides ( $n_g = c/v_g$ ),  $\varphi$  is the initial phase of the lightwave in optical waveguides ( $\varphi = k_m n_g y'$ ),  $D$  is the distance of the patches in the array structure, and  $n_0$  is the refractive index of the millimeter-wave in air (=1).

The proposed EMF sensor is an optical phase modulator, therefore the sensitivity or modulation efficiency,  $\Delta\phi$  is proportional to power ratio between lightwave carrier and sidebands, when  $\Delta\phi \ll 1$ . The modulation efficiency is calculated by the integration of millimeter-wave electric field as would be observed by the lightwave along the patches with orthogonal gaps, it can be expressed as following equations

from waveguide along  $x$ -axis:

$$\Delta\phi(\theta_x) = \frac{\pi r_{33} n_e^3}{\lambda} \Gamma \sum_{h=-N}^N \int_0^L E_{light}^h(x, \theta_x) dx \quad (5)$$

from waveguide along  $y$ -axis:

$$\Delta\phi(\theta_y) = \frac{\pi r_{33} n_e^3}{\lambda} \Gamma \sum_{h=-N}^N \int_0^L E_{light}^h(y, \theta_y) dy \quad (6)$$

where  $\lambda$  is the wavelength of lightwave propagating in the optical waveguides,  $r_{33}$  is the EO coefficient,  $n_e$  is the extraordinary refractive index of the substrate,  $\Gamma$  is a factor expressing the overlapping between the induced millimeter-wave and the lightwave electric field,  $L$  are the width of the patch electrodes as the interaction length of the millimeter-wave and lightwave electric field, and  $N$  is the number of gap-embedded patch electrodes in an array structure.

#### 4. Characterization of EMF Sensor

In the device experiment, the designed device was fabricated. First, a  $z$ -cut  $\text{LiNbO}_3$  wafer with a thickness of  $250\mu\text{m}$  was used. Then, orthogonal optical waveguides were fabricated on the EO crystal using titanium diffusion method with  $1100^\circ\text{C}$  for 10 hours. After that, a  $0.2\mu\text{m}$ -thick  $\text{SiO}_2$  buffer layer was deposited on the  $\text{LiNbO}_3$  wafer. An array of patches with gaps was fabricated on the  $\text{LiNbO}_3$  wafer with  $2\mu\text{m}$ -thick gold film using thermal vapor deposition, standard photo-lithography, and a lift-off methods. The optical waveguides were aligned precisely onto one side of the gap edges.

We have prepare also a ground metal on the bottom surface of a low- $k$  dielectric material. Then, the top surface of a low- $k$  dielectric material was covered with an optical adhesive for bonding process. In bonding process, the  $\text{LiNbO}_3$  wafer was flipped over with  $180$  degrees. So as the metal antennas become on the bottom surface of the  $\text{LiNbO}_3$  wafer. Then, the flipped  $\text{LiNbO}_3$  wafer was bonded to the low- $k$  dielectric material by exposing ultraviolet (UV) light. Finally, the  $250\mu\text{m}$ -thick  $\text{LiNbO}_3$  wafer was polished to the designed thickness of about  $70\mu\text{m}$  using a polishing machine with diamond slurry.

The fabricated EMF sensor was also cut and polished using dicing machine for lightwave couple between the fabricated optical waveguides with optical fibers. A photograph of the fabricated millimeter-wave EMF sensor is shown in Fig. 3.

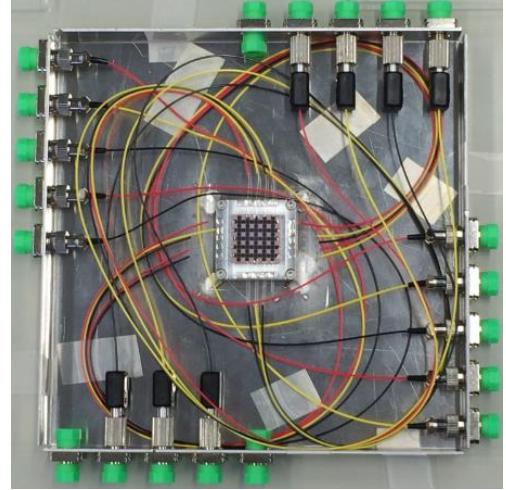


Fig. 3 A photograph of the fabricated EMF sensor coupled with optical fibers.

The fabricated EMF sensor characteristics were measured experimentally with a measurement setup as shown in Fig. 4. Lightwave of  $1.55\mu\text{m}$  operational wavelength from laser were propagated to optical fibers and coupled to the fabricated EMF sensor.  $40\text{GHz}$  millimeter-wave signal from a signal generator was amplified and irradiated to the fabricated EMF sensor using a horn antenna with  $\sim 20\text{mW}$  irradiation power. The output lightwave signals were measured using an optical spectrum analyzer (OSA).

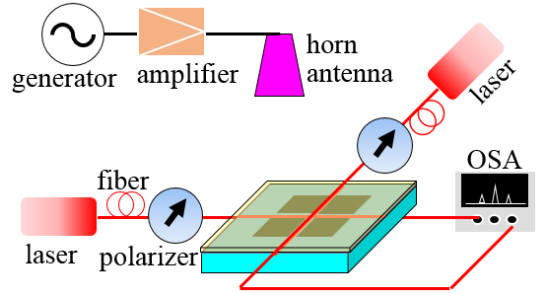


Fig. 4 Measurement setup for characterization of the fabricated EMF sensor.

Typical of the measured output lightwave spectra from two orthogonal waveguides are shown in Fig. 5 for variation of millimeter-wave polarization, when a  $34\text{GHz}$  wireless millimeter-wave signal was irradiated at the device at a normal irradiation angle. The optical sidebands were observed clearly when the millimeter-wave polarization is not parallel to the optical waveguides as shown in Fig. 5(a) and (c). They have about  $6\text{dB}$  difference due to  $45$  degree rotation of the millimeter-wave polarization. Almost no optical modulation is induced

when the millimeter-wave polarization is parallel to the optical waveguides as shown in Fig. 5(b).

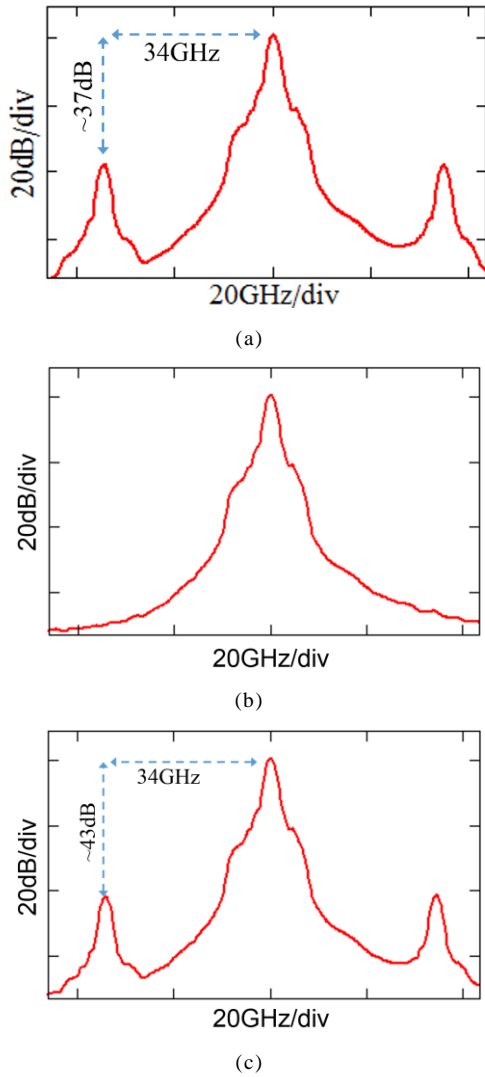


Fig. 5 Typical measured output lightwave spectra from the orthogonal waveguides, when the optical waveguide is (a) perpendicular, (b) parallel, and (c) 45 degree to the millimeter-wave polarization.

## 5. Demonstration of EMF Measurement

Figure 6 shows a setup of EMF measurement using the fabricated EMF sensor. Additional components with optical filters, optical amplifiers, and high-speed photodetectors were used. The optical filter were used for cutting one sideband and reducing ratio between optical carrier and sideband. The filtered lightwave signals were amplified using the optical amplifier. The modulated lightwave were detected by high-speed photo-detectors for reconvertng them to millimeter-wave. The reconverted millimeter-wave can be measured using millimeter-wave power meter, millimeter-wave spectrum analyzer, and

high-speed oscilloscope.

The typical measurement results of the reconverted millimeter-wave using spectrum analyzer is shown in Fig. 7. The measured millimeter-wave with carrier-to-noise ratio (CNR) of about 30dB was obtained. The millimeter-wave power of about -13dBm was also measured using power meter.

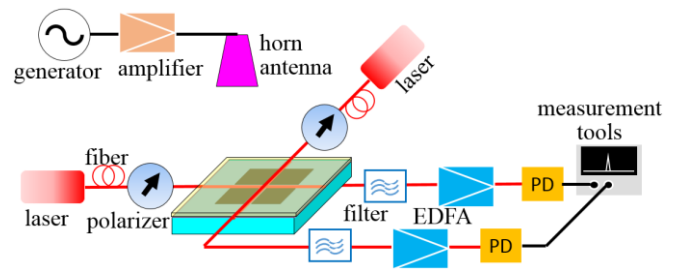


Fig. 6 Setup for millimeter-wave EMF measurement using the fabricated EMF sensor.

Based on that, the proposed millimeter EMF sensor using  $\text{LiNbO}_3$  optical modulators with patch antennas embedded with gaps can be used for measuring EMF characteristics of a DUT such as magnitude, phase, and polarization. The proposed EMF sensor has very low millimeter-wave loss and operated with no external power supply. However, sensitivity or efficiency of the sensor should be increased for obtaining precise measurement. Calibration of the fabricated EMF sensor must be also done for standardization.

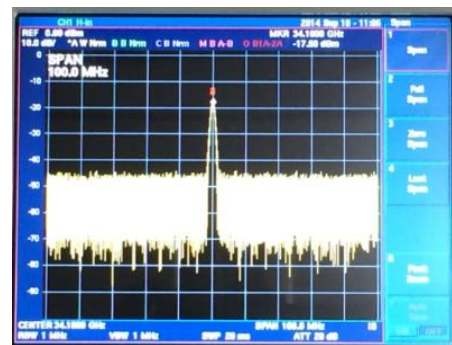


Fig. 7. Measured reconverted millimeter-wave using millimeter-wave spectrum analyzer.

## 6. Conclusion

Millimeter-wave EMF measurement based on a  $\text{LiNbO}_3$  optical modulator using patch antennas embedded with gaps was proposed. The millimeter-wave EMF sensor has simple and compact device structure. Detail analysis of the proposed EMF sensor for 40GHz

millimeter-wave bands was discussed in millimeter-wave and optical modulation analysis. Device experiment in fabrication and measurement were also reported. Based on the measurement results, the proposed EMF sensor can be used properly for identifying EMF radiated from a DUT. Magnitude, phase, and polarization of the millimeter-wave EMF can be observed. In this method, ROF technology was adopted for eliminating unwanted environmental noise and millimeter-wave loss.

Now we are still attempting to increase the sensitivity of the EMF sensor. Furthermore, broadband EMF sensor for millimeter-wave or terra-hertz bands will be also considered to realize. We believe that the EMF measurement for high operational frequency will be required soon, therefore the proposed device is promising for the EMF sensor.

### Acknowledgments

Authors would like thank to Dr. Hidehisa Shiomi from Osaka University Japan, Dr. Toshimasa Umezawa and Mr. Sinya Nakajima from National Institute of Information and Communications Technology (NICT) Japan for their constructive comments and suggestions during the discussion and helpful supports during the experiment in device fabrication and measurement.

Y. N. Wijayanto, A. Kanno, and T. Kawanishi would like thank to the Ministry of Internal Affairs and Communications, Japan, for the financial support partly through the project entitled "Research and Development of high-precision imaging technology using 90 GHz band linear cells" funded by the "Research and Development to Expand Radio Frequency Resources."

### References:

- [1] W.O. Henry, "Electromagnetic Compatibility Engineering," John Wiley & Sons, Inc, 2009.
- [2] I.F. Akyildiz, D.M. Gutierrez-Estevez, and E.C. Reyes, "The evolution to 4G cellular systems: LTE-Advanced," *Physical Communication*, vol. 3, pp. 217-244, 2010.
- [3] D. Morgan, "A Handbook for EMC Testing and Measurement," Inspec/Iee, 1994.
- [4] H.M. Pues, F.W. Trautnitz, "Design of modern EMC chambers for radiated EMC testing up to 18 GHz," IEEE International Symposium on Electromagnetic Compatibility, pp.72-77, 18-22 Aug 1997.
- [5] J. Kim, H. Kim, C. Song, I-M. Kim; Y. Kim; J. Kim, "Electromagnetic interference and radiation from wireless power transfer systems," IEEE International Symposium on Electromagnetic Compatibility (EMC), pp.171-176, 4-8 Aug. 2014.
- [6] Rec. ITU-R P.676-5, "Attenuation of atmospheric gases," 2001.
- [7] S.B. Poole, D.N. Payne, R.J. Mears, M.E. Fermann, R. Laming, "Fabrication and characterization of low-loss optical fibers containing rare-earth ions," *Journal of Lightwave Technology*, vol.4, no.7, pp.870-876, 1986.
- [8] T. Umezawa, A. Kanno, and T. Kawanishi, "EO-OE converting technologies for 90GHz radio over fiber system," The Third ENRI International Workshop on ATM/CNS, 2013.
- [9] A. Kanno and T. Kawanishi, "Broadband Frequency-Modulated Continuous-Wave Signal Generation by Optical Modulation Technique," *Journal of Lightwave Technology*, vol. 32, no. 20, pp.3566-3572, 2014.
- [10] S. Shinada, T. Kawanishi, T. Sakamoto, M. Andachi, K. Nishikawa, S. Kurokawa, and M Izutsu, "A 10-GHz Resonant-Type LiNbO<sub>3</sub> Optical Modulator Array," *IEEE Photonics Technology Letters*, vol.19, no.10, pp.735-737, May 2007.
- [11] H. Murata, N. Kohmu, Y. N. Wijayanto, and Y. Okamura, "Integration of Patch Antenna on Optical Modulators," *IEEE Photonic Society Newsletter*, vol. 28, no. 2, pp.4-7, April 2014.
- [12] R. Rodriguez-Berral, F. Mesa, D. R. Jackson, "Gap Discontinuity in Microstrip Lines: An Accurate Semi Analytical Formulation," *IEEE Transactions on Microwave Theory and Techniques*, vol.59, no.6, pp. 1441-1453, June 2011.
- [13] R. E. Newnham, Properties of Materials, New York: Oxford University Press Inc., 2005.
- [14] R. Garg, P. Bartia, I. Bahl, and A. Ittipiboon, Microstrip Antenna Design Handbook, Norwood: Artech House, Inc., 2001.
- [15] D. Sanchez-Hernandez, "Millimeter-wave dual-band microstrip patch antennas using multilayer GaAs technology," *IEEE Transactions on Microwave Theory and Techniques*, vol.44 no 9, pp. 1590-1593, 1996.
- [16] A. Yariv, Quantum Electronics, 3rd ed., Wiley, New York, 1989.